Biomedical Physics & Engineering Express

Endorsed by IPEM Institute of Physics and Engineering in Medicine

ACCEPTED MANUSCRIPT

Optimal Digital Filter Selection for Remote Photoplethysmography (rPPG) Signal Conditioning

To cite this article before publication: Saygun Guler *et al* 2023 *Biomed. Phys. Eng. Express* in press https://doi.org/10.1088/2057-1976/acaf8a

Optimal Digital Filter Selection for Remote Photoplethysmography (rPPG) Signal Conditioning

Saygun Guler [1 *], Ata Golparvar [1, 2], Ozberk Ozturk [1], Huseyin Dogan[3], Murat Kaya Yapici [1, 4, 5]
[1] Faculty of Engineering and Natural Sciences, Sabanci University, 34956 Istanbul, Turkey
[2] Integrated Circuit Laboratory, École Polytechnique Fédérale de Lausanne (EPFL), 2002 Neuchâtel, Switzerland
[3] Department of Computing and Informatics, Bournemouth University, BH12 5BB, UK
[4] Sabanci University Nanotechnology and Application Center, Sabanci University, 34956 Istanbul, Turkey
[5] Department of Electrical Engineering, University of Washington, 98195 Washington, USA
* Correspondence Author (saygun.guler@sabanciuniv.edu)

***Abstract*—Remote photoplethysmography (rPPG) using camera-based imaging has shown excellent potential recently in vital signs monitoring due to its contactless nature. However, the optimum filter selection for pre-processing rPPG data in signal conditioning is still not straightforward. The best algorithm selection improves the signal-to-noise ratio (SNR) and therefore improves the accuracy of the recognition and classification of vital signs. We recorded more than 300 temporal rPPG signals where the noise was not motion-induced. Then, we investigated the best digital filter in pre-processing temporal rPPG data and compared the performances of 10 filters with 10 orders each (i.e., a total of 100 filters). The performances are assessed using a signal quality metric on three levels. The quality of the raw signals was classified under three categories; Q1 being the best and Q3 being the worst. The results are presented in SNR scores, which show that the Chebyshev II orders of 2nd, 4th, and 6th perform the best for denoising rPPG signals.**

***Index Terms*—digital signal processing, heart rate, health monitoring, vital signs, human-computer interaction, photoplethysmography (PPG), image processing**

I. Introduction

Camera-based remote photoplethysmography (rPPG) is a powerful contactless alternative technique for vital signs monitoring which comes without any requirements for body-worn sensors (including wearables or skin-interfaced devices), cuffs, or cumbersome measurement tools that might induce medical risk or discomfort such as allergic reactions and pain [1]. In addition, unlike contact-based health monitoring systems, rPPG-based health monitoring devices may enable rapid, mass population vital sign screening like never before similar to matured body temperature mass screening solutions [2], [3].

In rPPG, the vital signs are extracted in real time by analyzing the frames of video recordings composed in the RGB color model. Even though rPPG and contact photoplethysmography (cPPG) exploit different wavelengths, their principles are similar in concept [4]. Analyzing the green channel in the frequency domain usually gives adequate information about heart rate depending on the external factors (e.g., lighting, imaging device) [5]. However, contactless techniques are not without their challenges. Like cPPG, rPPG applications might suffer from the noise induced by the image sensor (e.g., electronic shot noise, readout noise, flicker noise) or subject motion [6].

Numerous techniques have been proposed to improve the rPPG data quality, which in principle, all recreate the pulse signals from the RGB channels generated from the video frames. The most common technique is the Independent Component Analysis (ICA) for eliminating the noise from the contaminated signal where RGB channels are treated as statistical data sets [7]. The most prevalent component analysis method, Joint Approximation Diagonalization of Eigen-matrices (Jade)-ICA, was introduced in 2010 for a heart rate prediction study [8]. Later, a chrominance-based method was shown to be effective in motion-linked noise suppression [9]. It generates the pulse by creating orthogonal signal components directly from the RGB channels. Then the Spatial Subspace Rotation method (2SR) was shown to outperform ICA and chrominance-based methods in signal-to-noise ratio (SNR) analyses [10]. It derives pulse data by estimating the RGB subspace rotation and does not require apriori skin or pulse-related information. The signature blood volume pulse (PBV) method recreates the pulse signal by discriminating the distortions from its source using a signal component called 'signature' [11].

Besides those well-established techniques, researchers also proposed adaptive filters for various rPPG applications. A robust motion noise suppression technique was proposed by combining the chrominance-based method with an adaptive filter whose parameters are assigned via the least mean square algorithm [12]. An adaptive bandpass filter was implemented for noisy frequency domains analyzing a spectrogram of the pulse signal with a sliding time window [13]. Though primarily used in electrocardiography (ECG) applications, the wavelet filter was also adapted for the rPPG data taken from a webcam for suppressing the noise induced by subject motion, and light variations [14].

Frequency domain features in cPPG have long been proven to contain vital information related to heart rate and oxygen saturation [4]. Additionally, researchers have shown the morphological features to be helpful when measuring blood pressure (BP) with the aid of machine learning techniques [15], [16]. A few attempts have been made in rPPG to investigate this relation for BP using similar features [17], [18]. Even though those studies justify using morphological features directly in artificial neural networks, one must take

great care when conditioning the signals beforehand, as the filters strongly affect the dimensions and SNR score of the pulse signal. Most of the signal processing studies in remote imaging are focused on designing adaptive filters for motion-induced noise and on new pulse generation techniques for better assessment accuracy [19].

Many digital filters could be used in the pre-processing, and researchers have preferred various types for different application areas. A comprehensive filtering study on rPPG was needed to determine the most effective filter. An ideal filter in signal conditioning for denoising purposes should be examined for academic research and the commercial digital healthcare applications and software currently being developed.

This study narrows down the myriad alternatives of filters in removing unwanted noise induced by the video camera sensors and will allow us to observe the reactions of the filters applied upon different raw signal (not conditioned) quality scores. We present the performances of 100 filters applied to more than 300 temporal rPPG recorded in this study.

II. Methods

A. Research Model

A hundred digital filter performances on rPPG signals were ranked in this study, and an optimal one was proposed. The filters were applied to rPPG datasets generated from video frames. The study model was summarized as a flowchart in Figure 1. Region of interest (ROI) masks were manually marked for each individual before generating rPPG datasets as shown in Figure 2. Fourier analyses have been applied to the green channels of all eligible recordings.

Signal operations were carried out in custom-written MATLAB scripts (MathWorks, USA). rPPG pulse signals were generated as normalized raw green channel data by taking the spatial average of the ROI pixels in video frames since the green channel, amongst blue and green, carries the most robust information about heart rate [5]. No other processing technique was applied before the filtering. This is formalized in Equation 1 where $\mu(G_i)$ represents the temporal mean in the time domain.

$$G_n = -1 * \frac{G_i}{\mu(G_i)} \tag{1}$$

As this study focused on analyzing the performances of the selected digital filters in suppressing the sensor-induced noise but not motion, SNR was chosen as the only metric in performance evaluation. De Haan et al.'s method outputs a quality score in dB after calculating the energy around the harmonics [9]. This is formulated as in the following where $S(f)$ represents the spectrum and $U_t(f)$ represents the frequency range around harmonics.

$$Signal = \sum_{f=0.2}^{15} (U_t(f)S(f)) \tag{2}$$

$$Noise = \sum_{f=0.2}^{15} ((1 - U_t(f))(S(f))) \tag{3}$$

$$SNR\ score = 10\ log_{10}\left(\frac{Signal}{Noise}\right) \tag{4}$$

The recordings were first classified into three categories according to their unfiltered quality: Q1, Q2, and Q3. The Q1 category has 40, the Q2 category has 144, and the Q3 category has 137 recordings (321 in total). Each temporal dataset in Q1 has a raw signal-to-noise ratio (SNR) score of 4 dB or above and has a mean amplitude of 0.5 (RGB unit) or above. Each dataset in Q2 has an SNR score between 0-4 dB and has a mean amplitude below 0.5 (RGB unit). The signals in the Q3 category have all negative SNR scores. Figure 1 shows 15-second sample rPPG signals in three categories.

The study model adopted in this work was previously proposed in [20] by Liang et al. to cPPG data, and they presented their findings categorically. Therefore, it would be feasible to compare the performances of the digital filters applied in this particular trial and the reactions of cPPG and rPPG signals to those filters.

B. Experimental Setup and Data Collection

Seventeen participants were recruited for this study (7 females and 10 males). They had mixed skin tones and were aged between 22 and 38. Four hundred and eight videos were recorded with two commercial products: 204 via a CCD Sony DSCH300 and 204 via a CMOS iPad Pro 2017 (24 recordings for each participant: 2 video cameras, for each camera 2 light settings, for each setting 2 light colour, for each colour 3 illuminance levels, 2x2x2x3=24). Figure 3 shows the controlled environment with the equipment setup.

Eighty-seven recordings were dismissed from the database because the estimated HRs did not match the ground-truth values measured by a commercial pulse oximeter due to the low quality of raw RGB signals. We anticipate that this is due to the lack of ambient light and participants' dark skin tone. Each recording was in 30 fps, and video length was 30 seconds. Participants were asked to keep as still as possible while sitting, and were exposed to two different light settings where the sources were positioned firstly in the same level with the faces, and secondly the level above the faces directed downwards.

It was previously shown that even minimal illuminance intensity variations might affect the rPPG signal morphology [21]. With that being said, each lighting set contained three illuminance intensity levels for white and yellow LED spotlights (Neewer 480 LED Panel Light), respectively and separately to change the nature of the noise and diversify the data pool. Illuminance intensity levels were adjusted at 30-60-100 Lux when the source was at level with the participants' faces, and to 60-90-130 Lux when the source was positioned above the faces directed downward as depicted in Figure 3. These settings were chosen so that participants would not

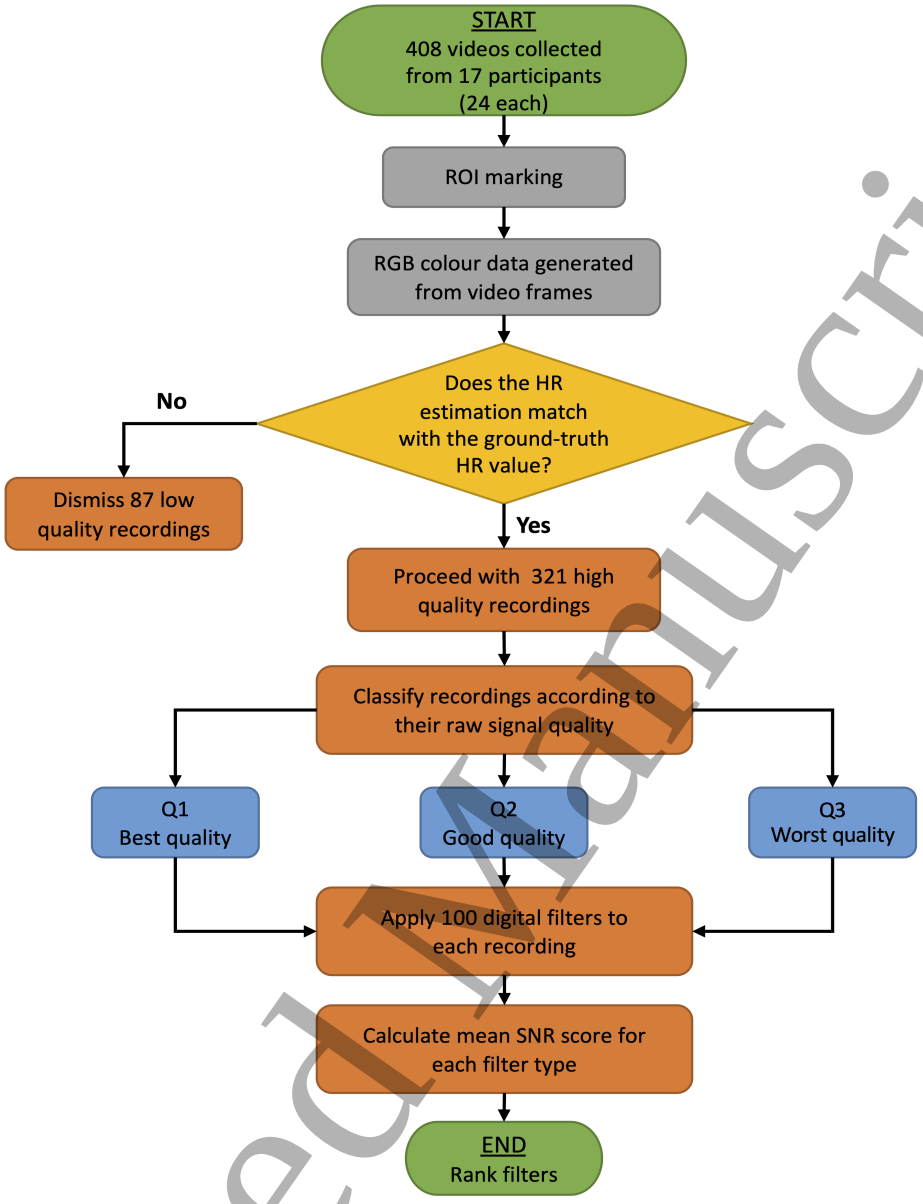

Fig. 1: Flowchart of the study model (Abbreviations: ROI-region of interest, RGB-red green blue, rPPG-remote photoplethysmography, SNR-signal-to-noise ratio

experience any eyestrain. The room had no light source except the controlled lighting equipment used for the study and had no window. Previous studies have shown that the cheeks are the best ROIs for generating rPPG data. [22], [23]. Since the participants were instructed not to move during video recordings, we manually marked the ROIs for each participant separately using *drawpolygon* and *poly2mask* functions in MATLAB without running an automated algorithm as illustrated in Figure 2.

C. Parameters Setting

A hundred different filters were applied to rPPG datasets that we recorded for this study, including wavelet, Savitzky-Golay, moving average, median, FIR least-square, Hamming, elliptic, Chebyshev, and Butterworth filters. These ten filter types are prevalently used in rPPG and cPPG research, as shown in Table I, especially in the pre-processing phase when raw data is conditioned before any morphology analyses.

Wavelet filters exploit discrete wavelet transform. We applied a wavelet filter with levels from 1 to 10. Savitzky-Golay filters smooth signals by fitting data to a low-degree polynomial. A 3rd order Savitzky-Golay filter was used with ten-odd consecutive frame lengths. As the name annotates, the moving average filters smooth signals by returning the average of neighboring elements in a dataset. We ran a moving average

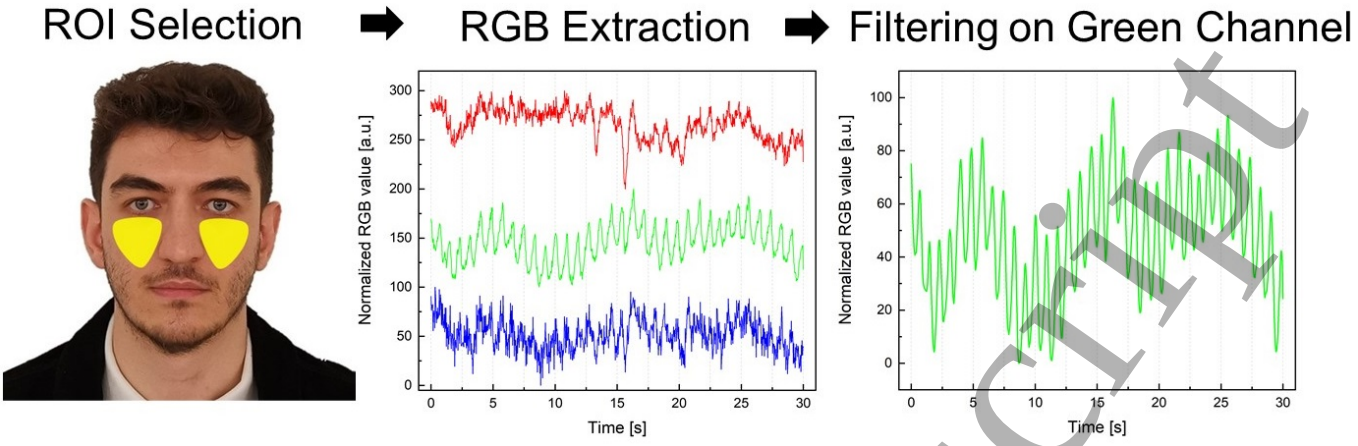

Fig. 2: ROIs are selected as both cheeks and marked in custom-written image processing scripts. Filtering experiments were conducted only on the green channel as it carries the most vital cardiac information.

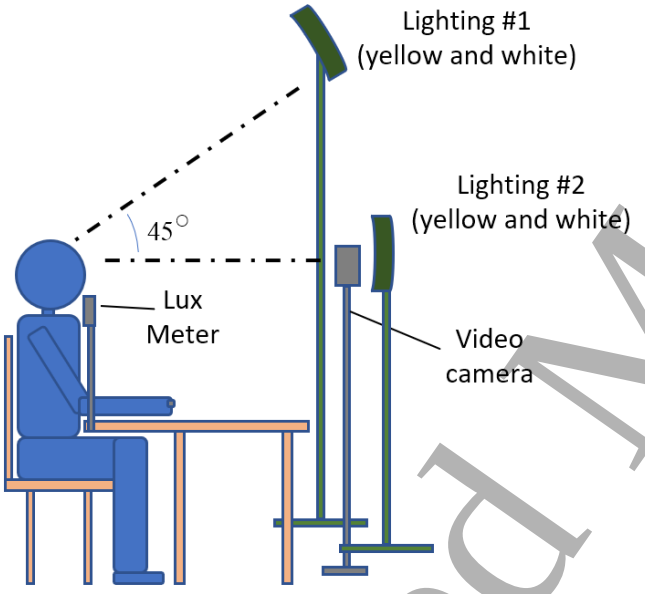

Fig. 3: Experimental setup contains 2 light settings, each setting contains 2 light colors, each color contains 3 illuminance intensity levels.

filter with ten-odd consecutive orders.

Median filters work with the same principle; they output the median value of neighboring elements. A median filter with ten-odd consecutive orders was used. Two finite impulse response (FIR) filters were implemented. FIR-hamming is a window-based filter, and the FIR-Least square uses the mean square error for filtering specifications. We applied both types with orders from 1 to 10.

Elliptic filters exhibit quick transitions on pass-band and stop-band. We implemented an elliptic filter with ten even consecutive orders. Two types of Chebyshev filters were also adopted. Type 1 Chebyshev filters are usually known to have steeper roll-off. We adopted both types with ten even consecutive orders. Type 2 Chebyshev was found to be the optimal rPPG filter according to the results obtained in this study, and its magnitude-squared transfer function is shown in Equation 5 [24].

$$|H_a(j\Omega)|^2 = \frac{\varepsilon^2 C_n^2(\Omega)}{1+\varepsilon^2 C_n^2(\Omega)} \tag{5}$$

where C_n represents Chebyshev polynomial and ε represents the ripple factor. Stop-band attenuation was set to 30 Hz. Butterworth filters, on the other hand, are the most common, and they are usually designed for flat frequency response in the pass-band; ten even consecutive orders were adopted. Passband ripple was set to 0.1 Hz. Band-pass borders were set in the range 0.83-1.66 Hz where applicable, which is equivalent to 50-100 beats per minute (bpm).

III. Results

SNR scores of the filtered signals were computed, then mean SNRs on Q1, Q2, and Q3 levels were calculated. The mean raw signal quality score for Q1 was 5.4 dB, for Q2 was 2.8 dB, and for Q3 was -2.65 dB. After filtering, no signal kept a negative quality score. Figure 4 shows the overall performance scores of all the filters on the horizontal axis. Most of the filters improved signal quality. However, the filters that have caused data loss (i.e., condition that a heart rate estimation is not possible in filtered signal) were marked as ”not applicable (NA)” in the figure. Namely, the highest three orders of Butterworth, Chebyshev I & II, and Elliptic filters are not usable in rPPG. We anticipate this is mainly due to suppression of the individual pulse waves when applied 16th orders of these filters and above. On the other hand, Chebyshev II, with 4th order, seems to be the optimal filter on all three levels.

IV. Discussion

Given that Elliptic and Chebyshev filters have sharp transition properties, these filters and Butterworth provide the best

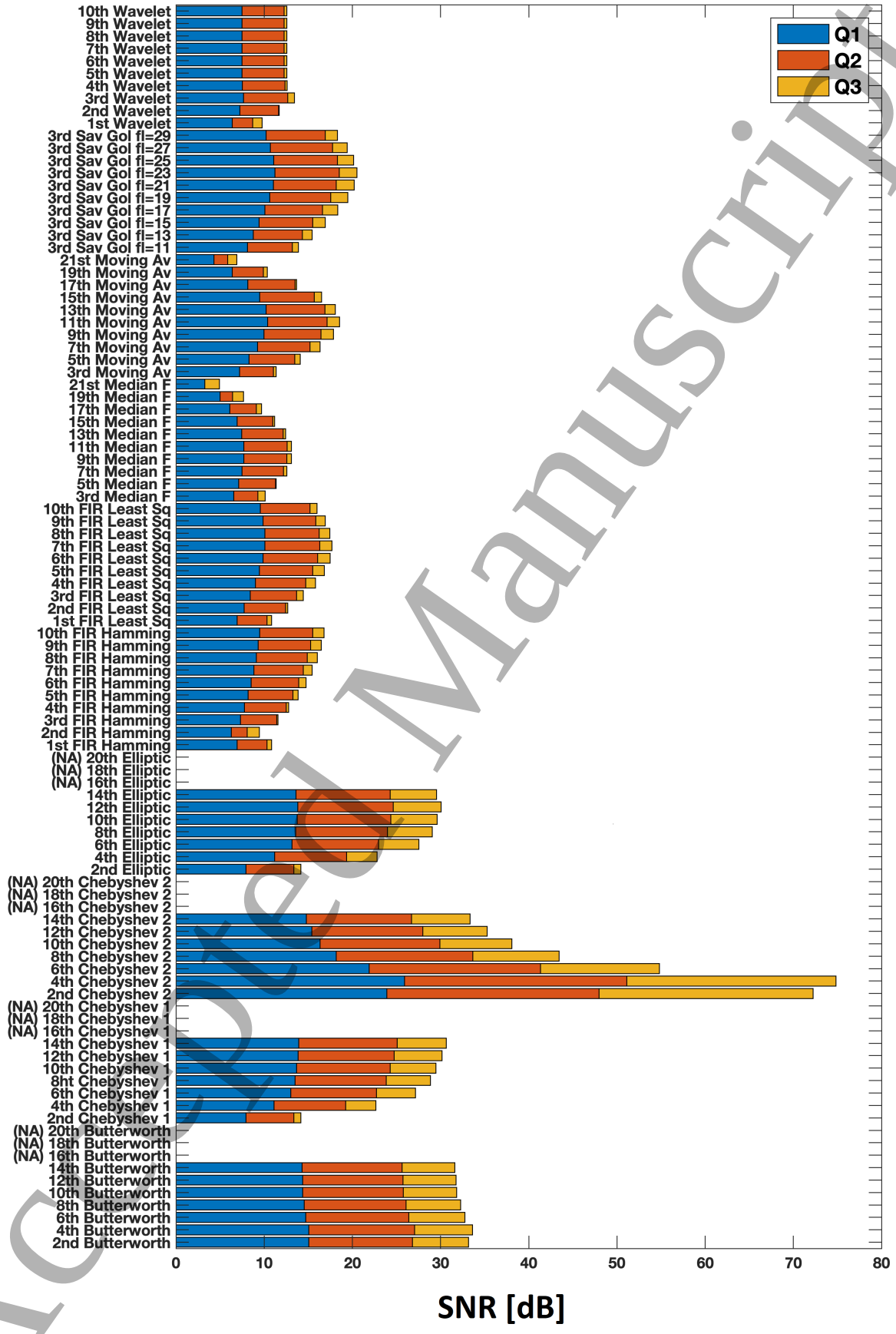

Fig. 4: All the tested filters' performances are shown. They were used in different settings for conditioning raw rPPG signals. SNR values of Q1, Q2, and Q3 are combined next to each other to indicate an augmentative signal quality score.

SNR scores. However, higher orders of these distort the data causing incorrect frequency extraction. Indeed, Butterworth had been previously reported to have performed relatively poorly in cPPG. In contrast, they might perform better than Elliptic filters in rPPG, especially with low orders. In the histogram of the results depicted in Figure 4, the only case in which the highest order of the relevant filter works better than its lower order was in the FIR-hamming filter. However, it might be due to our experiments' relatively high sampling rate (30 fps). Since this technique is window-based, it needs to be carefully handled as higher orders will suppress the pulse signals, leading to incorrect frequency analysis.

TABLE I: Recent rPPG studies which claimed to have used the most common undynamic filter types

Filter type	Paper reference
Butterworth	[5] [25] [26] [27] [28] [29] [30] [31] [32] [33] [34] [35] [36] [37]
Wavelet	[14] [38] [39] [40]
Elliptic	[41]
Moving Average	[42]
Sav-Gol	[43]
Hamming Window	[44]

The optimal filtering study conducted for cPPG has presented valuable results [20], and the signal quality indicator used was skewness which measures the symmetry (or asymmetry) of a given quantitative distribution [45]. Even though the skewness was shown to be the optimal signal quality indicator for cPPG, we preferred to use SNR instead in our rPPG experiments; because the high-frequency noise induced by the sensor and light variations needed to be assessed inclusively. The findings in these two studies have several similarities and significant performance differences. While the Chebyshev II and elliptic filters performed well in both cPPG and rPPG results, the difference between Chebyshev I and Butterworth stands out drastically. This is not surprising given that the lowest quality cPPG and rPPG signal natures are morphologically dissimilar.

Also, the Butterworth and Chebyshev filters perform well when removing high-frequency noise in PPG-shaped pulse waves. Thus, it increases the SNR but not skewness. As depicted in Table I, most rPPG studies have used Butterworth in their experiments. The moving average and median filters also performed relatively poorly in cPPG. However, the 11th order of these two exceptionally performed well in our experiment's Q2 group of rPPG signals. Another finding is that the window-based filters usually fail in bad-quality raw rPPG signals (i.e., Q3), including wavelet transforms. High-order Chebyshev's and elliptic filters can fix the Q3 signal quality at least 5 dB up.

V. Conclusion

Prior to this study, no critical comparative analysis has been made for ranking the most common unsophisticated filters in remote photoplethysmography (rPPG). Indeed, it was an open question that if the filters previously shown to be optimal for contact photoplethysmography (cPPG) would also be effective for rPPG signals obtained using commercial video cameras. Our analysis shows how a better filter selection would significantly impact the pre-processing phase of signal-processing rPPG pulses. The effects of the filter selected for the initial conditioning phase should be scrutinized to thoroughly understand the nature of the diagnostic features in rPPG morphology. Therefore, in this study, we reported the performances of 10 different filters with 10 orders each (i.e., 100 in total) and concluded that the Chebyshev type II filter with the order of 4 is the optimal filter for rPPG signal pre-processing applications. The existing noise in the raw signals was mainly induced by the sensor, not motion, as the subjects were asked to keep as still as possible in advance during the video recordings. As most rPPG studies stated that the Butterworth filters were applied in their experiments, a performance analysis needed to be conducted to see how it compares to similar filter types in suppressing the sensor noise. Window-based filters were shown to be disadvantageous, especially when working with raw rPPG signals of low quality (negative SNR).

VI. Acknowledgements

This study was partially funded by the Sabanci University research fund.

VII. Ethical Statement

All experiments were carried out in the physiology laboratory in Bournemouth University (BU). The Research Panel of BU approved the study. The study was performed in accordance with the ethical standards as laid down in the 1964 Declaration of Helsinki and its later amendments. The informed consents were obtained prior to the sessions from all participants. They all provided informed consent for publication of the images and relevant data that were collected during the experiments.

References

[1] M. S. van der Steen, J. W. Lenders, and T. Thien, "Side effects of ambulatory blood pressure monitoring:," *Blood Pressure Monitoring*, vol. 10, no. 3, pp. 151–155, Jun. 2005. [Online]. Available: http://journals.lww.com/00126097-200506000-00007

[2] S. Guler, A. Golparvar, O. Ozturk, and M. K. Yapici, "Ear Electrocardiography With Soft Graphene Textiles for Hearable Applications," *IEEE Sensors Letters*, vol. 6, no. 9, pp. 1–4, Sep. 2022. [Online]. Available: https://ieeexplore.ieee.org/document/9855407/

[3] G. Lippi, R. Nocini, C. Mattiuzzi, and B. M. Henry, "Is body temperature mass screening a reliable and safe option for preventing COVID-19 spread?" *Diagnosis*, vol. 9, no. 2, pp. 195–198, May 2022. [Online]. Available: https://www.degruyter.com/document/doi/10.1515/dx-2021-0091/html

[4] Y. Sun and N. Thakor, "Photoplethysmography Revisited: From Contact to Noncontact, From Point to Imaging," *IEEE Transactions on Biomedical Engineering*, vol. 63, no. 3, pp. 463–477, Mar. 2016. [Online]. Available: http://ieeexplore.ieee.org/document/7268900/

[5] W. Verkruysse, L. O. Svaasand, and J. S. Nelson, "Remote plethysmographic imaging using ambient light," *Optics Express*, vol. 16, no. 26, pp. 21 434–21 445, Dec. 2008.

[6] R. Sinhal, K. Singh, and M. M. Raghuwanshi, "An Overview of Remote Photoplethysmography Methods for Vital Sign Monitoring," in *Computer Vision and Machine Intelligence in Medical Image Analysis*, M. Gupta, D. Konar, S. Bhattacharyya, and S. Biswas, Eds. Singapore: Springer Singapore, 2020, vol. 992, pp. 21–31.

[7] G. R. Naik and D. K. Kumar, "An overview of independent component analysis and its applications," *Informatica*, vol. 35, no. 1, 2011.

[8] M.-Z. Poh, D. J. McDuff, and R. W. Picard, "Non-contact, automated cardiac pulse measurements using video imaging and blind source separation," *Optics Express*, vol. 18, no. 10, p. 10762, May 2010. [Online]. Available: https://www.osapublishing.org/abstract.cfm?URI=oe-18-10-10762

[9] G. de Haan and V. Jeanne, "Robust Pulse Rate From Chrominance-Based rPPG," *IEEE Transactions on Biomedical Engineering*, vol. 60, no. 10, pp. 2878–2886, Oct. 2013. [Online]. Available: https://ieeexplore.ieee.org/document/6523142/

[10] W. Wang, S. Stuijk, and G. de Haan, "A Novel Algorithm for Remote Photoplethysmography: Spatial Subspace Rotation," *IEEE Transactions on Biomedical Engineering*, vol. 63, no. 9, pp. 1974–1984, Sep. 2016. [Online]. Available: https://ieeexplore.ieee.org/document/7355301/

[11] G. de Haan and A. van Leest, "Improved motion robustness of remote-PPG by using the blood volume pulse signature," *Physiological Measurement*, vol. 35, no. 9, pp. 1913–1926, Sep. 2014.

[12] R.-Y. Huang and L.-R. Dung, "A motion-robust contactless photoplethysmography using chrominance and adaptive filtering," in *2015 IEEE Biomedical Circuits and Systems Conference (BioCAS)*. Atlanta, GA, USA: IEEE, Oct. 2015, pp. 1–4. [Online]. Available: http://ieeexplore.ieee.org/document/7348451/

[13] T. Blocher, K. Zhou, S. Krause, and W. Stork, "An Adaptive Bandpass Filter Based on Temporal Spectrogram Analysis for Photoplethysmography Imaging," in *2018 IEEE 20th International Workshop on Multimedia Signal Processing (MMSP)*. Vancouver, BC: IEEE, Aug. 2018, pp. 1–6. [Online]. Available: https://ieeexplore.ieee.org/document/8547129/

[14] F. Bousefsaf, C. Maaoui, and A. Pruski, "Continuous wavelet filtering on webcam photoplethysmographic signals to remotely assess the instantaneous heart rate," *Biomedical Signal Processing and Control*, vol. 8, no. 6, pp. 568–574, Nov. 2013. [Online]. Available: https://linkinghub.elsevier.com/retrieve/pii/S1746809413000840

[15] X. Xing and M. Sun, "Optical blood pressure estimation with photoplethysmography and FFT-based neural networks," *Biomedical Optics Express*, vol. 7, no. 8, p. 3007, Aug. 2016. [Online]. Available: https://www.osapublishing.org/abstract.cfm?URI=boe-7-8-3007

[16] M. Elgendi, Y. Liang, and R. Ward, "Toward Generating More Diagnostic Features from Photoplethysmogram Waveforms," *Diseases*, vol. 6, no. 1, p. 20, Mar. 2018. [Online]. Available: http://www.mdpi.com/2079-9721/6/1/20

[17] H. Luo, D. Yang, A. Barszczyk, N. Vempala, J. Wei, S. J. Wu, P. P. Zheng, G. Fu, K. Lee, and Z.-P. Feng, "Smartphone-Based Blood Pressure Measurement Using Transdermal Optical Imaging Technology," *Circulation: Cardiovascular Imaging*, vol. 12, no. 8, Aug. 2019. [Online]. Available: https://www.ahajournals.org/doi/10.1161/CIRCIMAGING.119.008857

[18] D. Djeldjli, F. Bousefsaf, C. Maaoui, F. Bereksi-Reguig, and A. Pruski, "Remote estimation of pulse wave features related to arterial stiffness and blood pressure using a camera," *Biomedical Signal Processing and Control*, vol. 64, p. 102242, Feb. 2021. [Online]. Available: https://linkinghub.elsevier.com/retrieve/pii/S1746809420303700

[19] Q. Xie, Q. Zhang, G. Wang, and Y. Lian, "Combining Adaptive Filter and Phase Vocoder for Heart Rate Monitoring Using Photoplethysmography During Physical Exercise," in *2018 40th Annual International Conference of the IEEE Engineering in Medicine and Biology Society (EMBC)*. Honolulu, HI: IEEE, Jul. 2018, pp. 3568–3571. [Online]. Available: https://ieeexplore.ieee.org/document/8512925/

[20] Y. Liang, M. Elgendi, Z. Chen, and R. Ward, "An optimal filter for short photoplethysmogram signals," *Scientific Data*, vol. 5, p. 180076, May 2018. [Online]. Available: http://www.nature.com/articles/sdata201876

[21] S. Guler, O. Ozturk, A. Golparvar, H. Dogan, and M. K. Yapici, "Effects of illuminance intensity on the green channel of remote photoplethysmography (rPPG) signals," *Physical and Engineering Sciences in Medicine*, Aug. 2022. [Online]. Available: https://link.springer.com/10.1007/s13246-022-01175-7

[22] G. Lempe, S. Zaunseder, T. Wirthgen, S. Zipser, and H. Malberg, "ROI Selection for Remote Photoplethysmography," in *Bildverarbeitung für die Medizin 2013*, H.-P. Meinzer, T. M. Deserno, H. Handels, and T. Tolxdorff, Eds. Berlin, Heidelberg: Springer Berlin Heidelberg, 2013, pp. 99–103.

[23] Sungjun Kwon, Jeehoon Kim, Dongseok Lee, and Kwangsuk Park, "ROI analysis for remote photoplethysmography on facial video," in *2015 37th Annual International Conference of the IEEE Engineering in Medicine and Biology Society (EMBC)*. Milan: IEEE, Aug. 2015, pp. 4938–4941. [Online]. Available: http://ieeexplore.ieee.org/document/7319499/

[24] N. A. Pashtoon, "IIR Digital Filters," in *Handbook of Digital Signal Processing*. Elsevier, 1987, pp. 289–357. [Online]. Available: https://linkinghub.elsevier.com/retrieve/pii/B9780080507804500096

[25] W. Wang and C. Shan, "Impact of makeup on remote-PPG monitoring," *Biomedical Physics & Engineering Express*, Oct. 2019. [Online]. Available: http://iopscience.iop.org/article/10.1088/2057-1976/ab51ba

[26] W. Wang, A. C. den Brinker, and G. de Haan, "Discriminative Signatures for Remote-PPG," *IEEE Transactions on Biomedical Engineering*, vol. 67, no. 5, pp. 1462–1473, May 2020. [Online]. Available: https://ieeexplore.ieee.org/document/8821386/

[27] U. Rubins, Z. Marcinkevics, I. Logina, A. Grabovskis, and E. Kviesis-Kipge, "Imaging photoplethysmography for assessment of chronic pain patients," in *Optical Diagnostics and Sensing XIX: Toward Point-of-Care Diagnostics*, G. L. Coté, Ed. San Francisco, United States: SPIE, Feb. 2019, p. 8. [Online]. Available: https://www.spiedigitallibrary.org/conference-proceedings-of-spie/10885/2508393/Imaging-photoplethysmography-for-assessment-of-chronic-pain-patients/10.1117/12.2508393.full

[28] D. McDuff and E. Blackford, "iPhys: An Open Non-Contact Imaging-Based Physiological Measurement Toolbox," *arXiv:1901.04366 [cs]*, Jan. 2019, arXiv: 1901.04366. [Online]. Available: http://arxiv.org/abs/1901.04366

[29] A. V. Moço, S. Stuijk, and G. de Haan, "New insights into the origin of remote PPG signals in visible light and infrared," *Scientific Reports*, vol. 8, no. 1, p. 8501, Dec. 2018. [Online]. Available: http://www.nature.com/articles/s41598-018-26068-2

[30] D. J. McDuff, E. B. Blackford, J. R. Estepp, and I. Nishidate, "A fast non-contact imaging photoplethysmography method using a tissue-like model," in *Optical Diagnostics and Sensing XVIII: Toward Point-of-Care Diagnostics*, G. L. Coté, Ed. San Francisco, United States: SPIE, Feb. 2018, p. 25. [Online]. Available: https://www.spiedigitallibrary.org/conference-proceedings-of-spie/10501/2285937/A-fast-non-contact-imaging-photoplethysmography-method-using-a-tissue/10.1117/12.2285937.full

[31] A. Trumpp, P. L. Bauer, S. Rasche, H. Malberg, and S. Zaunseder, "The value of polarization in camera-based photoplethysmography," *Biomedical Optics Express*, vol. 8, no. 6, p. 2822, Jun. 2017. [Online]. Available: https://opg.optica.org/abstract.cfm?URI=boe-8-6-2822

[32] S. Bobbia, R. Macwan, Y. Benezeth, A. Mansouri, and J. Dubois, "Unsupervised skin tissue segmentation for remote photoplethysmography," *Pattern Recognition Letters*, vol. 124, pp. 82–90, Jun. 2019. [Online]. Available: https://linkinghub.elsevier.com/retrieve/pii/S0167865517303860

[33] Z. Marcinkevics, U. Rubins, J. Zaharans, A. Miscuks, E. Urtane, and L. Ozolina-Moll, "Imaging photoplethysmography for clinical assessment of cutaneous microcirculation at two different depths," *Journal of Biomedical Optics*, vol. 21, no. 3, p. 035005, Mar. 2016.

[34] S. Fallet, V. Moser, F. Braun, and J.-M. Vesin, "Imaging Photoplethysmography: What are the Best Locations on the Face to Estimate Heart Rate?" in *Computing in Cardiology Conference (CinC)*, Vancouver, BC, 2016. [Online]. Available: http://infoscience.epfl.ch/record/222366

[35] Y. Sun, C. Papin, V. Azorin-Peris, R. Kalawsky, S. Greenwald, and S. Hu, "Use of ambient light in remote photoplethysmographic systems: comparison between a high-performance camera and a low-cost webcam," *Journal of Biomedical Optics*, vol. 17, no. 3, p. 037005, 2012.

[36] E. Jonathan and M. Leahy, "Investigating a smartphone imaging unit for photoplethysmography," *Physiological Measurement*, vol. 31, no. 11, pp. N79–N83, Nov. 2010. [Online]. Available: http://stacks.iop.org/0967-3334/31/i=11/a=N01?key=crossref.f67e9865c046430cf4e6477dbecf465e

[37] P. A. Shi, V. A. Peris, A. Echiadis, J. H. Zheng, Y. Zhu, P. Y. S. Cheang, and S. Hu, "Non-contact Reflection Photoplethysmography towards Effective Human Physiological Monitoring," 2010.

[38] Y. Wu, L. Kong, F. Chen, Y. Zhao, L. Dong, M. Liu, M. Hui, X. Liu, C. Li, and W. Wang, "Motion robust Imaging photoplethysmography in defocus blurring," in *Applications of Digital Image Processing XLII*, A. G. Tescher and T. Ebrahimi, Eds. San Diego, United States: SPIE, Sep. 2019, p. 4. [Online]. Available: https://www.spiedigitallibrary.org/conference-proceedings-of-spie/11137/2527655/Motion-robust-Imaging-photoplethysmography-in-defocus-blurring/10.1117/12.2527655.full

[39] Q. Fan and K. Li, "Non-contact remote estimation of cardiovascular parameters," *Biomedical Signal Processing and Control*, vol. 40, pp. 192–203, Feb. 2018. [Online]. Available: https://linkinghub.elsevier.com/retrieve/pii/S1746809417302318

[40] ——, "Noncontact Imaging Plethysmography for Accurate Estimation of Physiological Parameters," *Journal of Medical and Biological Engineering*, vol. 37, no. 5, pp. 675–685, Oct. 2017. [Online]. Available: http://link.springer.com/10.1007/s40846-017-0272-y

[41] E. B. Blackford and J. R. Estepp, "Using consumer-grade devices for multi-imager non-contact imaging photoplethysmography," G. L. Coté, Ed., San Francisco, California, United States, Feb. 2017, p. 100720P.

[42] X. Niu, X. Zhao, H. Han, A. Das, A. Dantcheva, S. Shan, and X. Chen, "Robust Remote Heart Rate Estimation from Face Utilizing Spatial-temporal Attention," in *2019 14th IEEE International Conference on Automatic Face & Gesture Recognition (FG 2019)*. Lille, France: IEEE, May 2019, pp. 1–8. [Online]. Available: https://ieeexplore.ieee.org/document/8756554/

[43] W. Sun, H. Wei, and X. Li, "No-contact heart rate monitoring based on channel attention convolution model," in *Eleventh International Conference on Graphics and Image Processing (ICGIP 2019)*, Z. Pan and X. Wang, Eds. Hangzhou, China: SPIE, Jan. 2020, p. 88. [Online]. Available: https://www.spiedigitallibrary.org/conference-proceedings-of-spie/11373/2557538/No-contact-heart-rate-monitoring-based-on-channel-attention-convolution/10.1117/12.2557538.full

[44] D. McDuff, S. Gontarek, and R. W. Picard, "Improvements in Remote Cardiopulmonary Measurement Using a Five Band Digital Camera," *IEEE Transactions on Biomedical Engineering*, vol. 61, no. 10, pp. 2593–2601, Oct. 2014. [Online]. Available: http://ieeexplore.ieee.org/document/6815662/

[45] M. Elgendi, "Optimal Signal Quality Index for Photoplethysmogram Signals," *Bioengineering*, vol. 3, no. 4, p. 21, Sep. 2016. [Online]. Available: http://www.mdpi.com/2306-5354/3/4/21